Medium-modified evolution of multiparticle production in jets in heavy-ion collisions.

Redamy Perez Ramos

Medium-modified evolution of multiparticle production in jets in heavy-ion collisions

Redamy Pérez-Ramos[1]

II. Institut für Theoretische Physik, Universität Hamburg

Luruper Chaussee 149, D-22761 Hamburg, Germany

Abstract: The energy evolution of medium-modified average multiplicities and multiplicity fluctuations in quark and gluon jets produced in heavy-ion collisions is investigated from a toy QCD-inspired model. In this model, we use modified splitting functions accounting for medium-enhanced radiation of gluons by a fast parton which propagates through the quark gluon plasma. The leading contribution of the standard production of soft hadrons is found to be enhanced by the factor $\sqrt{N_s}$ while next-to-leading order (NLO) corrections are suppressed by $1/\sqrt{N_s}$, where the nuclear parameter $N_s > 1$ accounts for the induced-soft gluons in the hot medium. The role of next-to-next-to-leading order corrections (NNLO) is studied and the large amount of medium-induced soft gluons is found to drastically affect the convergence of the perturbative series. Our results for such global observables are cross-checked and compared with their limits in the vacuum and a new method for solving the second multiplicity correlator evolution equations is proposed.

Keywords: perturbative Quantum Chromodynamics, jets, multiplicity, QGP

[1]E-mail: redamy@mail.desy.de

1 Introduction

The properties of quark and gluon jets are strongly established and carefully studied through well known QCD evolution equations [1] in e^+e^-, ep and hadron collision experiments. In the case of high energy nucleus-nucleus collisions, hard jets propagate in a medium with different properties from those of the vacuum. Recent experiments at the Relativistic Heavy Ion Collider (RHIC) have established a phenomenon of strong high-transverse momentum hadron suppression [2, 3], which supports the picture that hard partons going through dense matter suffer a significant energy loss prior to hadronization in the vacuum (for recent review see [4]).

Since little is known so far on jet evolution in QCD media, predictions for multiparticle production in such reactions could be carried out by using a toy QCD-inspired model introduced by Borghini and Wiedemann in [5]; it allows for analytical computations and may capture some important features of a more complete QCD description. In this model, the Dokshitzer-Gribov-Lipatov-Altarelli-Parisi (DGLAP) splitting functions $q \to gq$ and $g \to gg$ [1] of the QCD evolution equations were distorted so that the role of soft emissions was enhanced by multiplying the infra-red singular terms by the medium factor N_s:

$$\Phi_g^g(N_s, x) = \frac{N_s}{x} - (1-x)[2 - x(1-x)], \quad \Phi_q^g(N_s, x) = \frac{C_F}{N_c}\left(\frac{N_s}{x} - 1 + \frac{x}{2}\right),$$

where x is the fraction of the outgoing jet energy carried away by a single gluon. Thus, the leading singular terms of the splitting functions play a more important role; from the theoretical point of view it could be considered as a result of some effective Lagrangian, which would be responsible for processes in a dense nuclear environment. In the approach [6], the medium-modified splitting functions are directly related to the medium-induced gluon spectrum $dI^{\text{med}}/dxdE$ [8], where E is the initial energy of the emitting parton going through the medium. As compared to the Borghini-Wiedemann model, the medium modifications explicitly depend on the parton virtuality through the enhanced induced gluon spectrum. However, we use the simpler interpretation of the induced-medium modification of the Borghini-Wiedemann model [5], which was further discussed and used on the description of final state hadrons produced in heavy-ion collisions [7].

In this paper we are concerned with multiparticle production in quark and gluon jets $A = q, g$, produced in nucleus-nucleus collisions at very high energy. We make predictions at NLO and NNLO for the average multiplicities N_A, for the ratio $r = N_g/N_q$ and finally for the second multiplicity correlators $\langle N_A(N_A-1)\rangle/N_A^2$, which defines the width of the multiplicity distribution. Such observables are of great importance and have been largely studied in the vacuum from both theoretical [10–13] and experimental [14–19] points of view. The problem of medium-modified multiparticle production has also been considered in [21, 22] with fixed coupling constant.

The starting point of our analysis is the NLO or Modified-Leading-Logarithmic-Approximation (MLLA) evolution equations [1], which determine the jet properties at all energies together with the initial conditions at threshold at small x. Their solutions with medium-modified splitting functions can be resummed in powers of $\sqrt{\alpha_s/N_s}$ and the leading contribution can be represented as an exponential of the medium-modified anomalous dimension, which takes the N_s-dependence:

$$N_A \simeq \exp\left\{\int^Y \gamma_{\text{med}}\left(\alpha_s(Y)\right) dY\right\},$$

where $\gamma_{\rm med}(\alpha_s)$ can be expressed as a power series of $\sqrt{\alpha_s/N_s}$ in the symbolic form:

$$\gamma_{\rm med}\left(\alpha_s\right) \simeq \sqrt{N_s} \times \sqrt{\alpha_s}\left(1+\sqrt{\frac{\alpha_s}{N_s}}+\frac{\alpha_s}{N_s}+\ldots\right).$$

Within this logic, the leading double logarithmic approximation (DLA, $\mathcal{O}(\sqrt{N_s\alpha_s})$), which resums both soft and collinear gluons, and NLO (MLLA, $\mathcal{O}(\alpha_s)$), which resums hard collinear partons and accounts for the running of the coupling constant α_s, are complete. The DLA takes into account, as expected, the medium modification by enhancing the soft multiparticle production by a factor $\propto \sqrt{N_s}$, the MLLA terms, which are N_s-independent, takes into account the energy balance in the hard collinear parton splitting region as in the absence of the nuclear modification. However, this result depends on the definition of the medium-modified splitting functions. The next terms, which are NNLO or next-to-MLLA (NMLLA, $\mathcal{O}(\alpha_s^{3/2}/\sqrt{N_s})$) are not complete but they include an important contribution, which takes into account energy conservation and provide an improved behavior near threshold. With medium modification, the NMLLA terms take N_s-dependence, but this will be explained in the main core of the paper. This logic applies to each vertex of the cascade and the solution represents the fact that successive and independent partonic splittings inside the shower, which in this case concern both vacuum and medium-induced soft gluons, exponentiate with respect to the *evolution-time* variable Y ($dY = d\Theta/\Theta$), where $\Theta \ll 1$ is the angle between outgoing couples of partons. The choice of $Y \simeq \ln(\Theta)$ follows from Angular Ordering (AO) in intra-jet cascades; furthermore, the tree Feynman diagrams describing the process are at the heart of the *parton shower picture* [1]. Thus, the solutions of the equations incorporate the Markov chains of sequential angular ordered decays and $\gamma_{\rm med}$ determines, in this case, the rate of multiparticle production in the dense medium.

At the end of the cascading process inside the medium, partons hadronize in the vacuum. In order to obtain the hadronic spectra, we advocate for the Local Parton Hadron Duality (LPHD) hypothesis [23]: global and differential partonic observables can be normalized to the corresponding charged hadronic observables via a certain constant $\mathcal{K}$ that can be fitted to the data, i.e. $N_A^h = \mathcal{K} \times N_A$.

The paper is organized as follows:

- Section 2 presents a system of evolution equations with medium-modified splitting functions, which allows for the computation of the medium-modified average multiplicity and the medium-modified gluon to quark average multiplicity ratio at NLO and NNLO. We give predictions for the values $N_s = 1.6$ and $N_s = 1.8$, which may be realistic for RHIC and LHC phenomenology [5]. Moreover, we compare our results with previous predictions in the vacuum;
- in Section 3 we study the medium-modified second multiplicity correlator at NLO and NNLO. Accordingly, we give predictions for the same values of N_s and compare such predictions with the equivalent for the vacuum limit $N_s = 1$;
- in Section 4 we present our conclusions.

2 Evolution of the average multiplicity and gluon to quark average multiplicity ratio with energy loss

At MLLA the evolution of quantities with jet energy E and jet opening angle Θ is given by an evolution equation for the azimuthally averaged generating functional in the jet [1]. The evolution involves α_s, the running coupling constant of QCD:

$$\alpha_s \equiv \alpha_s(Q) = \frac{2\pi}{4N_c\beta_0 \ln\left(\frac{Q}{\Lambda}\right)}, \quad \beta_0 = \frac{1}{4N_c}\left(\frac{11}{3}N_c - \frac{4}{3}T_R\right), \tag{1}$$

where $Q = E\Theta$ is the maximum transverse momentum of the jet, $\Lambda \equiv \Lambda_{QCD}$ is the intrinsic scale of QCD, β_0 is the first term in the perturbative expansion of the $\beta-$function, N_c is the number of colors and $T_R = n_f/2$, where n_f is the number of quark flavors. In the leading DLA, α_s is linked to the anomalous dimension γ_0 of twist-2 operators by the formula:

$$\gamma_0^2 \equiv \gamma_0^2(Q) = 2N_c\frac{\alpha_s(Q)}{\pi} = \frac{1}{\beta_0(Y+\lambda)}, \quad Y = \ln\frac{Q}{Q_0}, \quad \lambda = \ln\frac{Q_0}{\Lambda}, \tag{2}$$

where Q_0 is the collinear cut-off parameter $k_T = E\Theta > Q_0$. The results depend on energy and angle only through the variable Y. For the sake of simplicity we also set $Y' = Y + \lambda$ in the following. The average multiplicity is obtained by integrating the one-particle single differential inclusive cross section over the energy fraction $x = e/E$

$$N_A(Y) = \int dx \left(\frac{1}{\sigma}\frac{d\sigma}{dx}\right).$$

For the medium-modified evolution of the average multiplicity in quark and gluon jets one obtains as a consequence of AO at MLLA, the coupled system of two evolution equations

$$\begin{aligned}\frac{d}{dY}N_g(Y) =& \int_0^1 dx\,\gamma_0^2(x)\left[\Phi_g^g(N_s,x)\left(N_g(Y+\ln x) + N_g(Y+\ln(1-x)) - N_g(Y)\right)\right.\\ &\left. + n_f\Phi_g^q(N_s,x)\left(N_q(Y+\ln x) + N_q(Y+\ln(1-x)) - N_g(Y)\right)\right],\end{aligned} \tag{3}$$

$$\frac{d}{dY}N_q(Y) = \int_0^1 dx\,\gamma_0^2(x)\left[\Phi_q^g(N_s,x)\left(N_g(Y+\ln x) + N_q(Y+\ln(1-x)) - N_q(Y)\right)\right] \tag{4}$$

with medium-modified splitting functions as suggested in [5] in the Borghini-Wiedemann model

$$\Phi_g^g(N_s,x) = \frac{N_s}{x} - (1-x)[2-x(1-x)], \quad \Phi_g^q(N_s,x) = \frac{1}{4N_c}[x^2 + (1-x)^2], \tag{5}$$

$$\Phi_q^g(N_s,x) = \frac{C_F}{N_c}\left(\frac{N_s}{x} - 1 + \frac{x}{2}\right), \tag{6}$$

which accounts for energy loss in the medium by enhancing the singular terms like $\Phi \approx N_s/x$ as $x \to 0$. The $g \to q\bar{q}$ splitting function as well as the regular parts of $g \to gg$ and $q \to g\bar{q}$ splitting functions are hard and provide collinear corrections, that is why these terms do not take N_s dependence.

2.1 MLLA evolution of the average multiplicity in the medium

For $Y \gg \ln x \sim \ln(1-x)$, $N(Y+\ln x)$ ($N(Y+\ln(1-x))$) can be replaced by $N(Y)$ in the hard partonic splitting region $x \sim 1$ ($1-x \sim 1$) (non-singular or regular parts of the splitting functions), while the dependence on $\ln x$ is kept on the singular one $\Phi(x) \approx N_s/x$ as it is performed in the vacuum. Furthermore, the integration over x can be replaced by the integration over $Y(x) = \ln\left(\frac{xE\Theta}{Q_0}\right)$

$$\int^1 \gamma_0^2(x)\frac{dx}{x} = \int^Y \gamma_0^2(Y(x))dY(x). \tag{7}$$

After applying the differential operator $\frac{d}{dY}$ to both members of the system (3,4) above, one is left with the approximate system of coupled equations,

$$\frac{d^2}{dY^2}N_g(Y) = \gamma_0^2\left(N_s - a_1\frac{d}{dY}\right)N_g(Y), \tag{8}$$

$$\frac{d^2}{dY^2}N_q(Y) = \frac{C_F}{N_c}\gamma_0^2\left(N_s - \tilde{a}_1\frac{d}{dY}\right)N_g(Y), \tag{9}$$

with the initial conditions at threshold $N_A^h(0) = 1$ and $N_A^{\prime h}(0) = 0$ and the hard constants

$$a_1 = \frac{1}{4N_c}\left[\frac{11}{3}N_c + \frac{4}{3}T_R\left(1 - 2\frac{C_F}{N_c}\right)\right], \qquad \tilde{a}_1 = \frac{3}{4}.$$

The quantum corrections $\propto a_1,\ \tilde{a}_1$ in (8,9) arise from the integration over the regular part of the splitting functions, they are $\mathcal{O}(\sqrt{\alpha}_s)$ suppressed and *partially* account for energy conservation as happens in the absence of the dense medium. Since only the DLA terms are medium-enhanced in (8,9), the hard constants are N_s-independent.

These equations can be solved by applying the inverse Mellin transform:

$$N_g(Y) = \int_C \frac{d\omega}{2\pi i}e^{\omega Y'}N_g(\omega) \tag{10}$$

to the self-contained gluonic equation (8), where the contour C lies to the right of all singularities of $N_G(\omega)$ in the complex plane. The running of the coupling constant $\alpha_s(Y)$, Eq. (2), is taken into account through the identity

$$\int_C \frac{d\omega}{2\pi i}Y' e^{\omega Y'}N_g(\omega) = -\int_C \frac{d\omega}{2\pi i}e^{\omega Y'}\left(2\omega N_g(\omega) + \omega^2\frac{d}{d\omega}N_g(\omega)\right).$$

Consequently, one is left with the following differential equation in Mellin space

$$\frac{1}{N_g}\frac{d}{d\omega}N_g(\omega) = -\frac{N_s}{\beta_0\omega^2} + \left(\frac{a_1}{\beta_0} - 2\right)\frac{1}{\omega}. \tag{11}$$

Solving (11) and using (10), one obtains

$$N_g(Y) \simeq \int_C \frac{d\omega}{2\pi i}\omega^{\frac{a_1}{\beta_0}-2}\exp\left(\omega Y' + \frac{N_s}{\beta_0\omega}\right). \tag{12}$$

The exact solution of (12) together with the initial conditions leads to a linear combination of two kinds of Bessel functions which resums the perturbative series at all powers of $\sqrt{\alpha}_s$ [1]. However, in this paper we are concerned with the asymptotic solution of the equation as $Y \gg 1$ ($E\Theta \gg Q_0$), that is

the high energy limit. Therefore, the Mellin transform (12) can be estimated by the steepest descent method. Indeed, the large parameter is Y' and the function in the exponent presents a saddle point at $\omega_0 = \sqrt{N_s/(\beta_0 Y')}$, such that the asymptotic solution reads

$$N_g^h(Y) \simeq \mathcal{K} \times Y'^{-\frac{\sigma_1}{\beta_0}} \exp \sqrt{\frac{4N_s}{\beta_0} Y'}, \tag{13}$$

where

$$\sigma_1 = \frac{a_1}{2} - \frac{\beta_0}{4}.$$

We also introduced, as stressed in the introduction, the LPHD normalization constant $\mathcal{K}$ [23], which accounts for hadronization effects outside the medium. The constant σ_1 is N_s-independent because it resums vacuum corrections. Therefore, the production of soft gluons in a dense medium becomes $\exp\left[2(\sqrt{N_s}-1)\sqrt{Y'/\beta_0}\right]$ higher than the standard production of soft gluons in the vacuum [1] and the factor $\sqrt{N_s}$ in (13) underlines the presence of the nuclear medium; this results has first been reported in [24]. From (13) one obtains the first and second logarithmic derivatives of N_g:

$$\frac{1}{N_g}\frac{dN_g}{dY} \equiv \frac{1}{N_q}\frac{dN_q}{dY} = \sqrt{N_s}\gamma_0 - \sigma_1\gamma_0^2, \quad \frac{1}{N_g}\frac{d^2N_g}{dY^2} \equiv \frac{1}{N_q}\frac{d^2N_q}{dY^2} = N_s\gamma_0^2. \tag{14}$$

The expression on the left hand side of (14) is nothing but the MLLA rate of multiparticle production with respect to the *evolution-time* variable $Y \simeq \ln(\Theta)$ in the medium, which we define as the medium-modified MLLA anomalous dimension:

$$\gamma_{\text{med}}(Y) \equiv \frac{1}{N_g}\frac{dN_g}{dY} = \sqrt{N_s}\gamma_0\left[1 - \sigma_1\frac{\gamma_0}{\sqrt{N_s}} + \mathcal{O}\left(\frac{\gamma_0^2}{N_s}\right)\right], \tag{15}$$

where N_s only affects, as expected, the leading double logarithmic term. From (13) and (15), one recovers the ansatz

$$N_g(Y) \simeq \exp\left(\int \gamma_{\text{med}}(Y)dY\right), \tag{16}$$

which we further improve in the next paragraph by adding higher order corrections. Finally, using (13) and (8,9), one obtains the solution for N_Q^h:

$$N_q(Y) = \frac{C_F}{N_c}\left[1 + (a_1 - \tilde{a}_1)\frac{\gamma_0}{\sqrt{N_s}}\right]N_g(Y) + \mathcal{O}\left(\frac{\gamma_0^2}{N_s}\right). \tag{17}$$

Therefore, we can introduce the medium-modified MLLA gluon to quark average multiplicity ratio $r = N_g/N_q = N_g^h/N_q^h$ in the form

$$r = r_0\left[1 - r_1\frac{\gamma_0}{\sqrt{N_s}} + \mathcal{O}\left(\frac{\gamma_0^2}{N_s}\right)\right], \qquad r_0 = \frac{N_c}{C_F}, \qquad r_1 = a_1 - \tilde{a}_1, \tag{18}$$

where the suppression factor $1/\sqrt{N_s}$ restricts the production of hard collinear partons as $N_s > 1$. We notice that (18) is identical to the expression with fixed coupling constant $\alpha_s(Y)$, where $Y = \ln(Q/Q_0)$ and $Q = E\Theta$ is the virtuality of the jet produced in the nucleus-nucleus reaction. This factor is found to suppress the hard correction $\mathcal{O}(\gamma_0)$ and therefore, r approaches its asymptotic DLA limit $r_0 = N_c/C_F$ when the coherent radiation of soft gluons is enhanced. Setting $N_s = 1$ in (18), one recovers the appropriate limits in the vacuum [1, 11, 25]. The constants entering in (13) and (18) are the same as those obtained in the vacuum and their values are displayed in Table 1.

n_f	r_1	σ_1
3	0.185	0.280
4	0.191	0.297
5	0.198	0.314

Table 1: Coefficients r_1 and σ_1.

2.2 Medium-modified equations and solutions at Next-to-MLLA

Previous MLLA results for the average multiplicities can be improved by further pushing the perturbative series in (3,4). We can include NNLO or NMLLA corrections of order $\mathcal{O}(\alpha_s)$, which are known to better account for energy conservation in the vacuum [12, 17, 20]. For this purpose, we replace $N(Y+\ln x)$ ($N(Y+\ln(1-x))$ by the Taylor expansion $N(Y)+\frac{d}{dY}N(Y)\ln x+\ldots$ ($N(Y)+\frac{d}{dY}N(Y)\ln(1-x)+\ldots$) and, as in section 2.1, we integrate over the non-singular parts of the splitting functions. We thus obtain the medium-modified NMLLA approximate system of two-coupled evolution equations

$$\frac{d^2}{dY^2}N_g(Y) \;=\; \gamma_0^2\left(N_s - a_1\left(\frac{d}{dY}-\beta\gamma_0^2\right)+a_2(N_s)\frac{d^2}{dY^2}\right)N_g(Y), \tag{19}$$

$$\frac{d^2}{dY^2}N_q(Y) \;=\; \frac{C_F}{N_c}\gamma_0^2\left(N_s - \tilde{a}_1\left(\frac{d}{dY}-\beta\gamma_0^2\right)+\tilde{a}_2(N_s)\frac{d^2}{dY^2}\right)N_g(Y), \tag{20}$$

with the new N_s-dependent constants

$$a_2(N_s)=\frac{67}{36}-N_s\frac{\pi^2}{6}-\frac{13}{18}\frac{T_R}{N_c}\frac{C_F}{N_c}+\frac{2}{3}\frac{T_R}{N_c}\frac{C_F}{N_c}\frac{(a_1-\tilde{a}_1)}{\sqrt{N_s}},\quad \tilde{a}_2(N_s)=\frac{7}{8}+\frac{C_F}{N_c}\left(\frac{5}{8}-N_s\frac{\pi^2}{6}\right).$$

The dependence of a_2 and $\tilde{a}_2$ on N_s follows from the singular term in the integral $N_s\int_0^1\frac{dx}{x}\ln(1-x)=-N_s\frac{\pi^2}{6}$ which also enhances (see below) the induced soft gluon radiation at the NNLO level. The term $\propto 1/\sqrt{N_s}$ in $a_2(N_s)$ was obtained by replacing (17) in the single logarithmic piece $\propto N_q$ in (3), while the term $\propto N_s$ in the equations (19,20) enhances the role of the leading DLA as in (8,9). As expected, one recovers the constants $a_2(N_s=1)=a_2$ and $\tilde{a}_2(N_s=1)=\tilde{a}_2$ obtained in the vacuum [20] when $N_s=1$. The terms proportional to these constants are known to better account for energy conservation in the partonic shower in the vacuum. Also note that the contributions $\propto a_1\beta_0$ and $\tilde{a}_1\beta_0$ cannot be neglected when performing predictions with running coupling coupling constant.

The system (19,20) can be solved by inserting the ansatz (16) in both sides of (19) with

$$\gamma_{\text{med}}(Y)=\sqrt{N_s}\gamma_0\left[1-\sigma_1\frac{\gamma_0}{\sqrt{N_s}}-\sigma_2(N_s)\frac{\gamma_0^2}{N_s}+\mathcal{O}\left(\frac{\gamma_0^3}{N_s^{3/2}}\right)\right], \tag{21}$$

where $\sigma_2(N_s)$ is the unknown coefficient to be determined. The medium-modified NMLLA anomalous dimension (21) has been inspired from the MLLA (15) where, in both cases, we make appear the rescaling of the coupling constant $\alpha_s\to\alpha_s/N_s$ in the series. After equating terms $\propto\gamma_0^2$ in the left and right hand sides of (19) we obtain the following value

$$\sigma_2(N_s)=-\frac{1}{2}\left(\frac{1}{2}a_1\beta_0+\frac{1}{4}a_1^2+N_sa_2(N_s)+\frac{3}{16}\beta_0^2\right), \tag{22}$$

such that after integrating (21) according to (16), the medium-modified NMLLA average multiplicity takes the simple form

$$N_g^h(Y) \simeq \mathcal{K} \times {Y'}^{-\frac{\sigma_1}{\beta_0}} \exp\left[\sqrt{\frac{4N_s}{\beta_0}Y'} + \frac{2\sigma_2(N_s)}{\sqrt{N_s\beta_0^3 Y'}}\right]. \tag{23}$$

The term $\propto \sigma_2(N_s)$ in (23) provides the NMLLA correction to N_G^h. As N_s increases, $\sigma_2(N_s)$ follows the leading behavior $\sigma_2(N_s) \simeq N_s^2$ (and the second factor in the exponent of (23) $\simeq N_s^{3/2}$) which enhances the production of induced soft gluons in the medium at the NNLO level. Setting $N_s = 1$ in (23) one recovers the value of this constant in the vacuum $\sigma_2(N_s = 1) \overset{n_f=3}{=} -0.378$ as given in [12]. Furthermore, setting $\beta_0 = 0$ in (22), the appropriate limit with fixed coupling constant $\alpha_s = const$ can be deduced.

We proceed to determine the medium-modified NMLLA gluon to quark average multiplicity ratio by subtracting (20) from (19), one has

$$\frac{d^2}{dY^2}\left(N_g - \frac{N_c}{C_F}N_q\right) = -(a_1 - \tilde{a}_1)\frac{d}{dY}(\gamma_0^2 N_g) - (\tilde{a}_2(N_s) - a_2(N_s))\gamma_0^2\frac{d^2 N_g}{dY^2}. \tag{24}$$

Applying the operators $\frac{d}{dY}$ and $\frac{d^2}{dY^2}$ to (20) and dropping corrections contributing beyond NMLLA, we obtain respectively

$$N_s\frac{d}{dY}(\gamma_0^2 N_g) = \frac{N_c}{C_F}\frac{d^3 N_q}{dY^3} + \tilde{a}_1\gamma_0^2\frac{d^2 N_g}{dY^2}, \quad N_s\gamma_0^2\frac{d^2 N_g}{dY^2} = \frac{N_c}{C_F}\frac{d^4 N_q}{dY^4}, \tag{25}$$

where we keep track of the nuclear factor N_s and the running of $\alpha_s(Y(x))$ in such a way that (24) can be rewritten in the form

$$N_g = \frac{N_c}{C_F}N_q - \frac{N_c}{C_F}\frac{(a_1 - \tilde{a}_1)}{N_s}\frac{dN_q}{dY} - \frac{N_c}{C_F}\left(\frac{\tilde{a}_1(a_1 - \tilde{a}_1)}{N_s^2} + \frac{(\tilde{a}_2(N_s) - a_2(N_s))}{N_s}\right)\frac{d^2 N_q}{dY^2},$$

after reassembling terms $\propto \frac{dN_q}{dY}$ and $\propto \frac{d^2 N_q}{dY^2}$. Using (14) together with the initial conditions at threshold yields for $r = N_g/N_q$ with NNLO accuracy

$$r = r_0\left[1 - r_1\frac{\gamma_0}{\sqrt{N_s}} - r_2(N_s)\frac{\gamma_0^2}{N_s} + \mathcal{O}\left(\frac{\gamma_0^3}{N_s^{3/2}}\right)\right], \tag{26}$$

where the coefficient r_2 is explicitly dependent on N_s through the formula

$$r_2(N_s) = (\tilde{a}_1 - \sigma_1)\, r_1 + (\tilde{a}_2(N_s) - a_2(N_s))N_s. \tag{27}$$

The dependence of $r_2(N_s)$ on β_0 in (26) underlines the account of the running coupling constant, setting $\beta_0 = 0$ the appropriate fixed coupling solution can be deduced. For $N_s = 1$, the appropriate limits in the vacuum are recovered [12], for example

$$r_2(N_s = 1) = (\tilde{a}_1 - \sigma_1)\, r_1 + (\tilde{a}_2(1) - a_2(1)) \overset{n_f=3}{=} 0.426.$$

We give the NMLLA coefficients $\sigma_2(N_s)$ and $r_2(N_s)$ defined in (23) and (26) as a function of N_s in Table 2.

As N_s increases, the $\mathcal{O}(\gamma_0/\sqrt{N_s})$ correction decreases, while the one $\mathcal{O}(\gamma_0^2/N_s)$ becomes sizable and decreases like $\simeq -N_s$. That is why it might be wondered whether the convergence of the perturbative series could be reached at a certain level of accuracy. Since the series widely oscillate at low energy scales, large terms $\propto \pi^2$ in $a_2(N_s)$ and $\tilde{a}_2(N_s)$ might spoil or drastically affect the trends obtained at MLLA. This kind of behavior has first been noticed in the Koba-Nielsen-Olsen (KNO) problem [28] in the vacuum.

n_f	$r_2(N_s)$	$\sigma_2(N_s)$
3	$0.087 - 0.027\sqrt{N_s} - 0.548N_s + 0.914N_s^2$	$-0.337 - 0.014\sqrt{N_s} - 0.850N_s + 0.822N_s^2$
4	$0.087 - 0.038\sqrt{N_s} - 0.494N_s + 0.914N_s^2$	$-0.319 - 0.019\sqrt{N_s} - 0.823N_s + 0.822N_s^2$
5	$0.087 - 0.049\sqrt{N_s} - 0.441N_s + 0.914N_s^2$	$-0.302 - 0.024\sqrt{N_s} - 0.797N_s + 0.822N_s^2$

Table 2: Coefficients $r_2(N_s)$ and $\sigma_2(N_s)$.

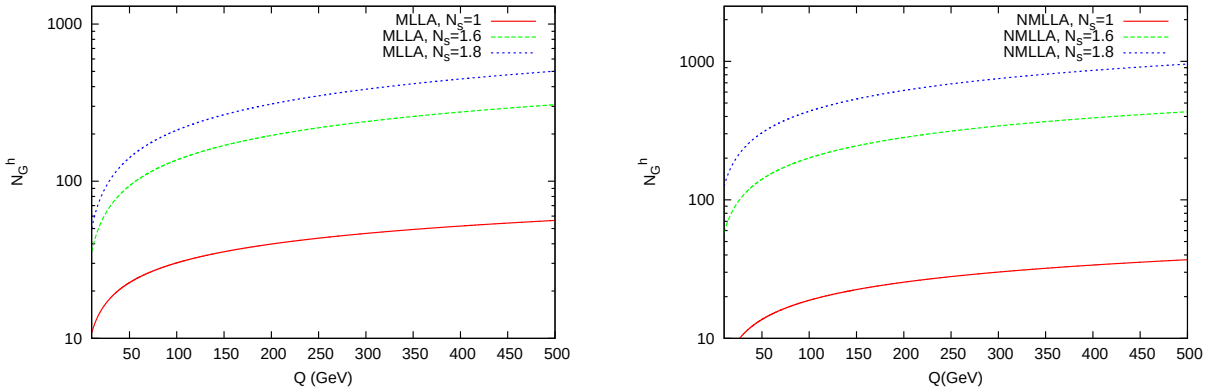

Figure 1: MLLA (13) and NMLLA (23) average multiplicity as a function of $Q = E\Theta$ in the vacuum ($N_s = 1$) and in the medium ($N_s = 1.6$ and $N_s = 1.8$).

2.3 NLO and NNLO results on N_g^h and r

Setting $n_f = 3$, we display in Fig. 1 our results for the medium-modified MLLA (13) and NMLLA (23) average multiplicity. We plot N_g^h in the range $10 \leq Q(\text{GeV}) \leq 500$, where $Q = E\Theta$ is the total virtuality of the jet related to Y in (2). We compare our results in the medium for $N_s = 1.6$ and $N_s = 1.8$ (see [5]) with predictions in the vacuum ($N_s = 1$), we set $Q_0 = \Lambda_{QCD} = 0.23$ GeV in the limiting spectrum approximation [12], and $\mathcal{K} = 0.2$ is taken from [12]. The values $N_s = 1.6$ and $N_s = 1.8$ in the medium may be realistic for RHIC and LHC phenomenology [5, 26]; the jet energy subrange $10 \leq Q(\text{GeV}) \leq 50$ displayed in Fig. 1 has been recently considered by the STAR collaboration, which reported the first measurements of charged hadrons and particle-identified fragmentation functions from p+p collisions [27] at $\sqrt{s_{\text{NN}}} = 200$ GeV. Finally, the jet energy range in the same figure, in particular for those values at $Q \geq 50$ GeV, will be reached at the LHC, i.e $Q = 100$ GeV is an accessible value in this experiment (see [5] and references therein).

Notice that at NMLLA, the increase of N_g^h with N_s is more substantial than at MLLA. The former is driven by the leading contribution to $\sigma_2(N_s)$: it increases like $\sigma_2(N_s) \simeq N_s^2$ (see Table 2) in the sub-leading piece of (23). In both resummations schemes we find, as expected from our calculations, that the production of soft hadrons increases as $N_s > 1$, which implies that the available phase space becomes restricted for the production of harder collinear hadrons.

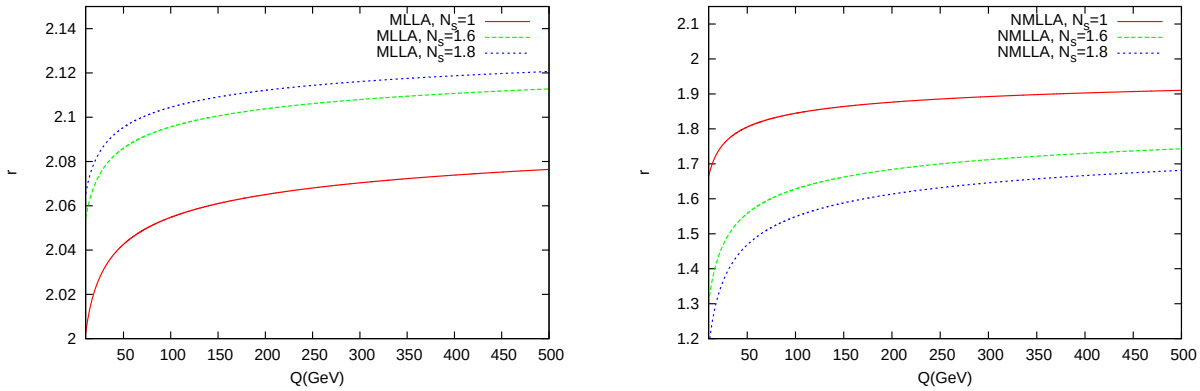

Figure 2: MLLA (18) and NMLLA (26) gluon to quark average multiplicity ratio as a function of $Q = E\Theta$ in the vacuum ($N_s = 1$) and in the medium ($N_s = 1.6$ and $N_s = 1.8$).

In Fig. 2, we display the medium-modified MLLA ratio $r = N_g/N_q$ (18) and the medium-modified NMLLA ratio as a function of $Q = E\Theta$. As expected from (18), as N_s increases, the $\mathcal{O}(\gamma_0)$ correction is suppressed by $1/\sqrt{N_s}$, the ratio approaches the DLA asymptotic regime $r_0 = N_c/C_F = 9/4$. At NMLLA, the previous trend goes in the opposite direction: one has indeed $-r_2(N_s) \simeq -N_s^2$ (see Table 2) in the $\mathcal{O}(\gamma_0^2/N_s)$ piece of (26), which is negative and sizable as N_s increases and, therefore, spoils the behavior obtained at MLLA signaling difficulties with perturbative theory in the medium. Indeed, sizable oscillations have been noticed in the perturbative series [13] and it turns out that they are wider in the medium than in the vacuum. For example, the NMLLA correction to r is $\sim 10\%$ for $N_s = 1$, and for $N_s = 1.8$ it is $\sim 40\%$. It should be noticed that every logarithmic derivative of N_A^h provides a half power of N_s to successive terms in the series in the form $\frac{d^n N}{dY^n} \approx (N_s\alpha_s)^{n/2}$ ($n = 1 \rightarrow$ MLLA, $n = 2 \rightarrow$ NMLLA...), such that the perturbative approach should fail as higher order terms are incorporated. Former statements suggest that by incorporating NMLLA and next-to-NMLLA (NNMLLA, see paragraph 3.4) corrections on an equal footing, the MLLA behavior can be recovered. We conclude from this analysis that MLLA provides a more realistic physical picture of the softening of jets than NMLLA. Therefore, either the incorporation of NNMLLA terms or the exact numerical solution of the evolution equations [7, 29], which exactly accounts for the running of α_s and the energy balance, is required. In [21], a numerical solution of the equations was provided with fixed coupling constant α_s, and the results are shown to follow our MLLA expectations as N_s increases.

Finally, in both MLLA and NMLLA, the gluon jets are still more active than the quark jets in producing secondary particles and the shape of the curves are roughly identical; however, these characteristics prove not to be very sensitive to N_s.

3 Medium-modified evolution for the second multiplicity correlator

The second multiplicity correlator was first considered in [11] at MLLA and later in [13] at NMLLA. It is defined in the form $N_A^{(2)} = \langle N_A(N_A - 1)\rangle$ in gluon ($A = g$) and quark ($A = q$) jets. The normalized second multiplicity correlator defines the width of the multiplicity distribution and is related

to its dispersion $D_A^2 = \langle N_A(N_A-1)\rangle - N_A^2$ by the formula

$$D_A^2 = (A_2-1)N_A^2 + N_A. \tag{28}$$

The second multiplicity correlators normalized to their own squared average multiplicity are

$$G_2 = \frac{\langle N_g(N_g-1)\rangle}{N_g^2}, \quad Q_2 = \frac{\langle N_q(N_q-1)\rangle}{N_q^2}, \tag{29}$$

inside a gluon and a quark jet respectively. These observables are obtained by integrating the double differential inclusive cross section over the energy fractions $x_1 = e_1/E$ and $x_2 = e_2/E$

$$\langle N_A(N_A-1)\rangle = \iint dx_1 dx_2 \left(\frac{1}{\sigma}\frac{d^2\sigma}{dx_1 dx_2}\right)_A.$$

The correlators are $\mathcal{K}$-independent and provide a pure test of multiparticle dynamics. However, important disagreements with e^+e^- data [16] indicates that non-trivial hadronization effects may play a significant role. The treatment of this observable with full account of perturbative and non-perturbative ingredients is not available yet. Therefore, we study the variation of this observable as $N_s > 1$ with respect to the limit in the vacuum $N_s = 1$ and do not compare our results with e^+e^- data [16]. The medium-modified system of two-coupled evolution equations for this observable follows from the MLLA master equation for the azimuthally averaged generating functional and can be written in the convenient form

$$\begin{aligned}\frac{d}{dY}(N_g^{(2)} - N_g^2) = \int_0^1 dx\gamma_0^2\Phi_g^g \Big[N_g^{(2)}(Y+\ln x) + \Big(N_g^{(2)}(Y+\ln(1-x)) - N_g^{(2)}(Y)\Big) \\ + \Big(N_g(Y+\ln x) - N_g(Y)\Big)\Big(N_g(Y+\ln(1-x)) - N_g(Y)\Big)\Big] \\ + n_f\int_0^1 dx\gamma_0^2\Phi_g^q \Big[2\Big(N_q^{(2)}(Y+\ln x) - N_q^2(Y+\ln x)\Big) - \Big(N_g^{(2)}(Y) - N_g^2(Y)\Big) \\ + \Big(2N_q(Y+\ln x) - N_g(Y)\Big)\Big(2N_q(Y+\ln(1-x)) - N_g(Y)\Big)\Big],\end{aligned} \tag{30}$$

$$\begin{aligned}\frac{d}{dY}(N_q^{(2)} - N_q^2) = \int_0^1 dx\gamma_0^2\Phi_q^g \Big[N_g^{(2)}(Y+\ln x) + \Big(N_q^{(2)}(Y+\ln(1-x)) - N_q^{(2)}(Y)\Big) \\ + 2\Big(N_g(Y+\ln x) - N_q(Y)\Big)\Big(N_q(Y+\ln(1-x)) - N_q(Y)\Big)\Big],\end{aligned} \tag{31}$$

which proves to be more suitable for obtaining analytical solutions in the following. We use a new method to compute solutions at MLLA and NMLLA by replacing $N_A^{(2)} = A_2 N_A^2$ on both sides of the expanded equations at $x \sim 1-x \sim 1$. This observable is less inclusive than the average multiplicity, it can indeed be derived from the two-particle four-momentum correlation [30] in the shower. The medium-modified formulæ (16), (18) and (26) will be used in this analysis.

3.1 MLLA approximation

For $Y \gg \ln x \sim \ln(1-x)$ in the system above (30,31), $N(Y+\ln x)$ ($N(Y+\ln(1-x))$) and $N^{(2)}(Y+\ln x)$ ($N^{(2)}(Y+\ln(1-x))$) can be replaced by $N(Y)$ and $N^{(2)}(Y)$ respectively in the hard partonic splitting region $x \sim 1-x \sim 1$, while the dependence on $\ln x$ is kept on the singular one ($x \to 0$). The medium-modified MLLA approximate system of two-coupled evolution equations for the second

multiplicity correlator reads

$$\frac{d^2}{dY^2}\left(N_g^{(2)}-N_g^2\right)=\gamma_0^2\left(N_s-a_1\frac{d}{dY}\right)N_g^{(2)}+(a_1-b_1)\gamma_0^2\frac{d}{dY}N_g^2, \tag{32}$$

$$\frac{d^2}{dY^2}\left(N_q^{(2)}-N_q^2\right)=\frac{C_F}{N_c}\gamma_0^2\left(N_s-\tilde{a}_1\frac{d}{dY}\right)N_g^{(2)}, \tag{33}$$

where the new hard constant is:

$$b_1=\frac{1}{4N_c}\left[\frac{11}{3}N_c-4\frac{T_R}{N_c}\left(1-2\frac{C_F}{N_c}\right)^2\right].$$

The constant N_s only affects the leading double logarithmic term of the equations. The terms proportional to a_1, (a_1-b_1) and $\tilde{a}_1$ are hard vacuum corrections which *partially* account for energy conservation, indeed $\gamma_0^2\frac{dN}{dY}\approx\sqrt{N_s}\gamma_0^3$ and the relative correction to DLA is $\mathcal{O}(\sqrt{\alpha_s/N_s})$. As before, the hard constants are, as expected, N_s-independent. Moreover, these sub-leading contributions have the same form as those describing the two-particle correlation [30].

3.1.1 Medium-modified G_2 at MLLA and expansion in $\mathcal{O}(\gamma_0/\sqrt{N_s})$

Setting $N_g^{(2)}=G_2N_g^2$ in (32), the system can be solved iteratively by considering terms up to $\mathcal{O}(\alpha_s^{3/2})$ in the left and right hand sides of (32). Thus, the l.h.s. of (32) writes in the form

$$\frac{d^2}{dY^2}\left(N_g^{(2)}-N_g^2\right)=\frac{d^2G_2}{dY^2}N_g^2+2\frac{dG_2}{dY}\frac{d}{dY}N_g^2+(G_2-1)\frac{d^2}{dY^2}N_g^2. \tag{34}$$

Hereafter, in all sub-leading terms, we can replace G_2 by a constant $G_2=G_2^{\rm DLA}=const$, while the terms involving N_g should be computed by using (13), thus

$$\frac{d^2}{dY^2}\left(N_g^{(2)}-N_g^2\right)=\gamma_0^2N_s(G_2-1)\left[4-(4a_1-\beta_0)\frac{\gamma_0}{\sqrt{N_s}}\right]N_g^2 \tag{35}$$

while the r.h.s. reads

$$\left[\left(N_s\gamma_0^2-a_1\gamma_0^2\frac{d}{dY}\right)G_2+(a_1-b_1)\gamma_0^2\frac{d}{dY}\right]N_g^2 \;=\; \gamma_0^2N_s(G_2-1)N_g^2+N_s\gamma_0^2\left[1-\left(\frac{2}{3}a_1+2b_1\right)\frac{\gamma_0}{\sqrt{N_s}}\right]N_g^2. \tag{36}$$

Equating (35) and (36) the exact MLLA solution of (32) reads

$$G_2-1=\frac{1-\delta_1\frac{\gamma_0}{\sqrt{N_s}}}{3-\delta_2\frac{\gamma_0}{\sqrt{N_s}}}, \tag{37}$$

where

$$\delta_1=\left(\frac{2}{3}a_1+2b_1\right),\quad \delta_2=(4a_1-\beta_0).$$

Setting $\gamma_0/\sqrt{N_s}\to 0$ in (37) one recovers the DLA N_s-independent value $G_2^{\rm DLA}=4/3$. Then, expanding (37) in the form $1+\gamma_0/\sqrt{N_s}$, one recovers the result from [11] for $N_s=1$

$$G_2-1\approx\frac{1}{3}-c_1\frac{\gamma_0}{\sqrt{N_s}}+\mathcal{O}\left(\frac{\gamma_0^2}{N_s}\right), \tag{38}$$

where the linear combination of color factors reads

$$c_1=-\frac{2}{9}a_1+\frac{1}{9}\beta_0+\frac{2}{3}b_1=\frac{1}{4N_c}\left(\frac{55}{9}-4\frac{T_R}{N_c}+\frac{112}{9}\frac{T_R}{N_c}\frac{C_F}{N_c}-\frac{32}{3}\frac{T_R}{N_c}\frac{C_F^2}{N_c^2}\right). \tag{39}$$

3.1.2 Medium-modified Q_2 at MLLA and expansion in $\mathcal{O}(\gamma_0/\sqrt{N_s})$

Inserting (37), $N_q^{(2)} = Q_2 N_q^2$ and using the MLLA expression for the ratio (17) in (33), it is straightforward to obtain

$$\frac{Q_2 - 1}{G_2 - 1} = \frac{N_c}{C_F}\left[1 + \frac{3}{2}(b_1 - a_1)\frac{\gamma_0}{\sqrt{N_s}} + \mathcal{O}\left(\frac{\gamma_0^2}{N_s}\right)\right]. \tag{40}$$

Expanding (40) in the form $1 + \gamma_0/\sqrt{N_s}$ and setting $N_s = 1$, one recovers the result from [11] in the vacuum. Indeed,

$$Q_2 - 1 \approx \frac{N_c}{C_F}\left(\frac{1}{3} - \tilde{c}_1\frac{\gamma_0}{\sqrt{N_s}}\right) + \mathcal{O}\left(\frac{\gamma_0^2}{N_s}\right), \tag{41}$$

where, in agreement with [11], we obtain the combination of color factors

$$\tilde{c}_1 = \frac{5}{18}a_1 + \frac{1}{6}b_1 + \frac{1}{9}\beta_0 = \frac{1}{4N_c}\left(\frac{55}{9} + \frac{4}{9}\frac{T_R}{N_c}\frac{C_F}{N_c} - \frac{8}{3}\frac{T_R}{N_c}\frac{C_F^2}{N_c^2}\right). \tag{42}$$

In Table 3 we display $\tilde{c}_1$ together with c_1 (39) for $n_f = 3, 4, 5$. As for the medium-modified MLLA

n_f	c_1	$\tilde{c}_1$
3	0.485	0.495
4	0.477	0.491
5	0.469	0.486

Table 3: Coefficients c_1 and $\tilde{c}_1$.

expression $r = N_g/N_q$ (18), hard corrections to the MLLA second multiplicity correlators G_2 and Q_2 are suppressed by the factor $1/\sqrt{N_s}$, while the leading double logarithmic terms ($\gamma_0/\sqrt{N_s} \to 0$) remain unchanged and equal the vacuum result

$$A_2 = 1 + \frac{N_c}{3C_A}, \quad A = g\ (C_g = N_c), \quad A = q\ (C_q = C_F). \tag{43}$$

Thus, our MLLA predictions for the medium-modified second multiplicity correlators follow the characteristics of the jet quenching.

3.2 Next-to-MLLA evolution equations for the multiplicity correlator

To obtain the equations we proceed like in paragraph 2.2 and use results from subsection 3.1. Indeed, by further pushing the perturbative series, one can improve the account of the energy balance. We replace, in the hard splitting region $Y \gg \ln x \sim \ln(1-x)$, $N(Y + \ln x)$ ($N(Y + \ln(1-x))$) and $N^{(2)}(Y + \ln x)$ ($N^{(2)}(Y + \ln(1-x))$) by $N(Y) + \frac{d}{dY}N(Y)\ln x \ldots$ ($N(Y) + \frac{d}{dY}N(Y)\ln(1-x)\ldots$) and $N^{(2)}(Y) + \frac{d}{dY}N^{(2)}(Y)\ln x \ldots$ ($N^{(2)}(Y) + \frac{d}{dY}N^{(2)}(Y)\ln(1-x)\ldots$) respectively in the system (30,31), while the dependence on $\ln x$ is kept on the singular piece N_s/x. After integrating the regular

terms over x, the medium-modified NMLLA approximate system of two-coupled evolution equations for the gluon and quark multiplicity correlator reads

$$\frac{d^2}{dY^2}\left(N_g^{(2)}-N_g^2\right)=\gamma_0^2\left(N_s-a_1\left(\frac{d}{dY}-\beta_0\gamma_0^2\right)+a_2'(N_s)\frac{d^2}{dY^2}\right)N_g^{(2)} \tag{44}$$
$$+\gamma_0^2\left((a_1-b_1)\left(\frac{d}{dY}-\beta_0\gamma_0^2\right)+b_2(N_s)\frac{d^2}{dY^2}\right)N_g^2$$
$$+\gamma_0^3\,b_3(N_s)\frac{d}{dY}\left(N_g^{(2)}-N_g^2\right),$$
$$\frac{d^2}{dY^2}\left(N_q^{(2)}-N_q^2\right)=\frac{C_F}{N_c}\gamma_0^2\left(N_s-\tilde{a}_1\left(\frac{d}{dY}-\beta_0\gamma_0^2\right)+\tilde{a}_2(N_s)\frac{d^2}{dY^2}\right)N_g^{(2)}, \tag{45}$$

where the term $\propto b_3$ follows from the MLLA result (40),

$$N_q^{(2)}-N_q^2=\frac{C_F}{N_c}\left[1+\left(\frac{1}{2}a_1-2\tilde{a}_1+\frac{3}{2}b_1\right)\frac{\gamma_0}{\sqrt{N_s}}\right]\left(N_g^{(2)}-N_g^2\right).$$

The constants are the following:

$$a_2'(N_s)=a_2(N_s)-\frac{2T_R}{3N_c}\frac{C_F}{N_c}\frac{r_1}{\sqrt{N_s}}, \tag{46}$$
$$b_2(N_s)=\frac{T_R}{3N_c}\frac{C_F}{N_c}\left[\frac{13}{3}\left(1-\frac{C_F}{N_c}\right)-2\left(1-2\frac{C_F}{N_c}\right)\frac{r_1}{\sqrt{N_s}}\right], \tag{47}$$
$$b_3(N_s)=\frac{T_R}{3N_c}\frac{C_F}{N_c}\left(\frac{r_1}{\sqrt{N_s}}+3\frac{(b_1-\tilde{a}_1)}{\sqrt{N_s}}\right). \tag{48}$$

The terms $\propto\ a_1\beta_0,\ a_2'(N_s),\ (a_1-b_1)\beta_0,\ b_2(N_s),\ b_3(N_s)$ in (44) and the ones $\propto\ \tilde{a}_1\beta_0,\ \tilde{a}_2(N_s)$ in (45) are $\mathcal{O}(\gamma_0^2)$ corrections which better account for energy conservation. We remind that $\frac{d^nN}{dY^n}\simeq\mathcal{O}((N_s\alpha_s)^{n/2})$ and that terms $\propto\beta_0$ arise from the running of the coupling constant $\alpha_s(Y)$. Moreover, these constants take N_s-dependence for the reasons explained in section 2.2.

3.2.1 Medium-modified G_2 at NMLLA and expansion in $\mathcal{O}(\gamma_0/\sqrt{N_s})$

Setting $N_g^{(2)}=G_2N_g^2$ in (44), the equation can be solved iteratively by making use of (21), the MLLA formula (38) for G_2 and the leading DLA limit $G_2^{\rm DLA}=4/3$; moreover, we expand the series up to terms $\mathcal{O}(\alpha_s^2)$. The l.h.s. of (44) can therefore be written in the form,

$$l.h.s.=\gamma_0^2(G_2-1)\left[4N_s-(8\sigma_1+\beta_0)\sqrt{N_s}\gamma_0+2\left(\sigma_1(2\sigma_1+\beta_0)-4\sigma_2(N_s)\right)\gamma_0^2\right]N_g^2 \tag{49}$$
$$+\,2\beta_0c_1\gamma_0^4N_g^2.$$

The r.h.s. reads

$$r.h.s.=\gamma_0^2\left[N_s(G_2-1)+N_s-2\left(\frac{1}{3}a_1+b_1\right)\sqrt{N_s}\gamma_0+\left(\frac{1}{3}a_1+b_1\right)(2\sigma_1+\beta_0)\gamma_0^2\right. \tag{50}$$
$$\left.+\,2\left(\frac{1}{3}b_3(N_s)+a_1\frac{c_1}{\sqrt{N_s}}\right)\sqrt{N_s}\gamma_0^2+4\left(\frac{4}{3}a_2'(N_s)+b_2(N_s)\right)N_s\gamma_0^2\right]N_g^2.$$

Equating (49) and (50) we find the new exact NMLLA solution of (44),

$$G_2-1=\frac{1-\delta_1\frac{\gamma_0}{\sqrt{N_s}}+\delta_3(N_s)\frac{\gamma_0^2}{N_s}}{3-\delta_2\frac{\gamma_0}{\sqrt{N_s}}+\delta_4(N_s)\frac{\gamma_0^2}{N_s}}, \tag{51}$$

where the following combinations of color factors have been written in the form

$$\delta_3(N_s) = \left(\frac{1}{3}a_1 + b_1\right)(2\sigma_1 + \beta_0) + 2\left(\frac{1}{3}b_3(N_s) + \frac{c_1}{\sqrt{N_s}}(a_1 - \beta_0)\right)\sqrt{N_s} \tag{52}$$

$$+ 4\left(\frac{4}{3}a_2'(N_s) + b_2(N_s)\right)N_s, \tag{53}$$

$$\delta_4(N_s) = 2\left(\sigma_1(2\sigma_1 + \beta_0) - 4\sigma_2(N_s)\right). \tag{54}$$

When the MLLA coefficients δ_1, δ_2 and NMLLA $\delta_3(N_s)$ and $\delta_4(N_s)$ are evaluated in the vacuum ($N_s = 1$) for $n_f = 3$, we find respectively $\delta_1 = 2.453$, $\delta_2 = 2.991$, $\delta_3(1) = 2.818$ and $\delta_4(1) = 3.766$. In particular, $\delta_1 \sim \delta_3(1)$ while the NMLLA $\delta_4(1)$ becomes bigger than the MLLA δ_2. It was shown in the KNO problem that MLLA corrections increase like $\sim k\sqrt{\alpha_s}$ ($k = 2$) while NMLLA like $\sim k^2\alpha_s$ ($k^2 = 4$) as the rank of the correlator, which coincides with the number of particles triggered in the shower, increases [28]. It may be the reason why sizable NMLLA coefficients are found in this picture. Moreover, as the rank k of the correlator increases, $\mathcal{O}(\sqrt{\alpha_s})$ corrections become of the same order of magnitude than the leading DLA and perturbation theory fails. Therefore and in general, MLLA and NMLLA corrections for the less inclusive multiplicity correlator of any rank k are more sizable than those of the more inclusive average multiplicity. That is the reason for, the exact numerical solution of the evolution equations [7, 29] becomes interesting.

Expanding (51) in $\gamma_0/\sqrt{N_s}$ in the form $1 + \gamma_0/\sqrt{N_s} + \gamma_0^2/N_s$, we obtain

$$G_2 - 1 = \frac{1}{3} - c_1\frac{\gamma_0}{\sqrt{N_s}} + c_2(N_s)\frac{\gamma_0^2}{N_s} + \mathcal{O}\left(\frac{\gamma_0^3}{N_s^{3/2}}\right) \tag{55}$$

where

$$c_2(N_s) = \frac{1}{27}\left(\delta_2(N_s)^2 - 3\delta_4(N_s) - 3\delta_1(N_s)\delta_2(N_s) + 9\delta_3(N_s)\right). \tag{56}$$

Setting $N_s = 1$ in (56) and taking $n_f = 3, 4, 5$, we recover the values $c_2(1) = 0.0372, 0.0609, 0.0838$ obtained in the vacuum [13]. Moreover, in (55), the sign of successive terms change as higher order corrections are added to the series. Consequently, it should be wondered whether this result can drastically be affected as higher order terms are incorporated to the series at current energy scales. The highest energy scales reached at the LHC and measured by the ALICE and CMS experiments at CERN will provide more reliable comparisons with our predictions than current experimental studies at RHIC.

3.2.2 Medium-modified Q_2 at NMLLA and expansion in $\mathcal{O}(\gamma_0/\sqrt{N_s})$

The solution of (45) can also be obtained by setting $N_q^{(2)} = Q_2 N_q^2$ in the equation, using (51) and taking the MLLA formula for G_2 (41), one has

$$l.h.s. = 2\beta_0\frac{N_c}{C_F}\tilde{c}_1\gamma_0^4 N_Q^2 + \gamma_0^2(Q_2 - 1)\left(4N_s - \delta_2\sqrt{N_s}\gamma_0 + \delta_4(N_s)\gamma_0^2 - 4\beta_0 r_1\gamma_0^2\right)N_q^2, \tag{57}$$

and

$$r.h.s. = \frac{C_F}{N_c}\gamma_0^2\left(N_s G_2 - \frac{8}{3}\sqrt{N_s}\tilde{a}_1\gamma_0 + 2\left(\frac{2}{3}\tilde{a}_1(2\sigma_1 + \beta_0) + \tilde{a}_1 c_1 + \frac{8}{3}\tilde{a}_2(N_s)N_s\right)\gamma_0^2\right)N_g^2. \tag{58}$$

After equating (57) and (58) we obtain the new exact analytical solution of (45)

$$Q_2 - 1 = \frac{N_c}{C_F}\left(\frac{G_2 - \tilde{\delta}_1\frac{\gamma_0}{\sqrt{N_s}} + \tilde{\delta}_3(N_s)\frac{\gamma_0^2}{N_s}}{4 - \tilde{\delta}_2\frac{\gamma_0}{\sqrt{N_s}} + \tilde{\delta}_4(N_s)\frac{\gamma_0^2}{N_s}}\right)\frac{r^2}{r_0^2}, \tag{59}$$

where (see (26))

$$\frac{r}{r_0} = 1 - r_1 \frac{\gamma_0}{\sqrt{N_s}} - r_2(N_s)\frac{\gamma_0^2}{N_s}.$$

Moreover,

$$\tilde{\delta}_1 = \frac{8}{3}\tilde{a}_1 = 2, \quad \tilde{\delta}_2 = \delta_2, \tag{60}$$

$$\tilde{\delta}_3(N_s) = 2\left(\frac{2}{3}\tilde{a}_1(2\sigma_1 + \beta_0) + \tilde{a}_1 c_1 - \beta_0 \tilde{c}_1 + \frac{8}{3}\tilde{a}_2(N_s)N_s\right), \tag{61}$$

$$\tilde{\delta}_4(N_s) = \delta_4(N_s) - 4\beta_0 r_1, \tag{62}$$

and G_2 should be taken from (51). As before, the size of NMLLA coefficients $\tilde{\delta}_3(N_s)$ and $\tilde{\delta}_4(N_s)$ in the vacuum are quite sizable, for $n_f = 3$ one has indeed, $\tilde{\delta}_3(1) = 3.598$ and $\tilde{\delta}_4(1) = 3.210$, which are close to $k^2 = 4$, where $k = 2$ labels the rank of the second multiplicity correlator.

Performing the same expansion in $\gamma_0/\sqrt{N_s}$ we obtain the result

$$Q_2 - 1 \approx \frac{N_c}{C_F}\left(\frac{1}{3} - \tilde{c}_1\frac{\gamma_0}{\sqrt{N_s}} + \tilde{c}_2(N_s)\frac{\gamma_0^2}{N_s}\right) + \mathcal{O}\left(\frac{\gamma_0^3}{N_s^{3/2}}\right), \tag{63}$$

where the expression for $\tilde{c}_2(N_s)$ follows from (59):

$$\tilde{c}_2(N_s) = \frac{1}{12}\left(\frac{\delta_2^2(N_s)}{4} - \tilde{\delta}_4(N_s)\right) - \frac{\delta_2(N_s)}{16}\left(c_1 + 2 + \frac{8}{3}r_1\right) \tag{64}$$

$$+ \frac{1}{4}(c_2(N_s) + \tilde{\delta}_3(N_s)) + \frac{r_1}{2}(c_1 + 2) - \frac{1}{3}(2r_2(N_s) - r_1^2). \tag{65}$$

Accordingly, setting $N_s = 1$ in (64), we find the values in the vacuum $\tilde{c}_2(1) = 0.215, 0.222, 0.229$ respectively for $n_f = 3, 4, 5$ like in [13]. The sign of successive terms added to the series (63) shows the wide oscillating property. We give the values of $c_2(N_s)$ and $\tilde{c}_2(N_s)$ in Table 4.

n_f	$c_2(N_s)$	$\tilde{c}_2(N_s)$
3	$-0.258 - 0.016\sqrt{N_s} + 2.505N_s - 2.193N_s^2$	$-0.168 + 0.005\sqrt{N_s} + 1.962N_s - 1.584N_s^2$
4	$-0.236 - 0.022\sqrt{N_s} + 2.513N_s - 2.193N_s^2$	$-0.146 + 0.007\sqrt{N_s} + 1.946N_s - 1.584N_s^2$
5	$-0.215 - 0.029\sqrt{N_s} + 2.521N_s - 2.193N_s^2$	$-0.126 + 0.009\sqrt{N_s} + 1.930N_s - 1.584N_s^2$

Table 4: Coefficients $c_2(N_s)$ and $\tilde{c}_2(N_s)$.

3.3 NLO and NNLO results on G_2 and Q_2

The MLLA and NMLLA predictions for $G_2(Q)$ (55) and $Q_2(Q)$ (63) are depicted respectively in Fig. 3 and Fig. 4. At MLLA, the second multiplicity correlator increases as $N_s > 1$ and approaches the asymptotic regime $A_2 = 1 + \frac{N_c}{3C_A}$. Indeed, as for the MLLA ratio $r(N_s)$ (18), the hard corrections $\mathcal{O}(\gamma_0)$ are

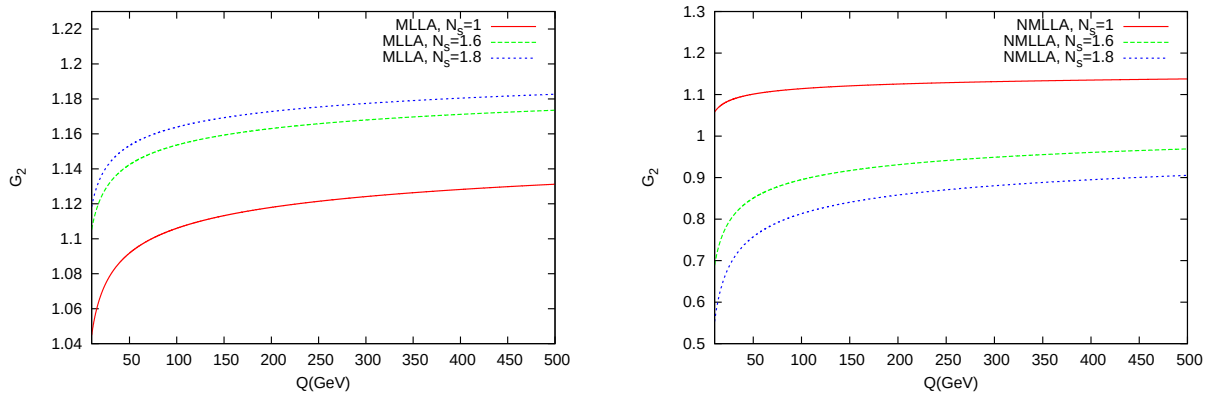

Figure 3: MLLA (38) and NMLLA (55) second multiplicity correlator inside a gluon jet as a function of $Q = E\Theta$ in the vacuum ($N_s = 1$) and in the medium ($N_s = 1.6$ and $N_s = 1.8$).

suppressed by $1/\sqrt{N_s}$, such that the production of soft and collinear hadrons is enhanced, while that of hard collinear hadrons is more restricted. As before, these results provide evidence for the softening of jets in the nuclear medium. However, the NMLLA results (55,63) follow the behavior described in section 2.3 for $r(N_s)$. As $N_s > 1$, the correlators decrease, one finds indeed the rough dependence $c_2(N_s) \simeq -N_s^2$, $\tilde{c}_2(N_s) \simeq -N_s^2$ (see Table 4), which in both cases leads to the unavoidable decrease of A_2 as N_s increases. This result follows from the wide oscillating property of the perturbative series: it is wider in the medium than in the vacuum. That is the reason why, the more physical MLLA trends can be recovered either by incorporating higher order terms or by numerically solving the evolution equations (30,31) like in [7, 29].

Another interesting feature of these observables concerns the shape of the curves. They are roughly identical and do not prove to depend on the medium parameter N_s. Moreover, there exists evidence for a flattening of the slopes as the jet hardness $Q = E\Theta$ increases for $N_s \geq 1$ (vacuum and medium). This kind of scaling behavior is known as the KNO scaling: it was discovered by Polyakov in quantum field theory [31] and experimentally confirmed by e^+e^- measurements [16] for the second and higher order multiplicity correlators. This phenomenon implies a jet energy independence of the normalized multiplicity correlators, which is not affected by N_s neither at MLLA nor at NMLLA.

3.4 Role of higher order corrections

In this paragraph we comment on some progresses that could be carried out beyond the NMLLA approximation. We take the much simpler example of the gluon to quark average multiplicity ratio and give the rough dependence of the third coefficient $r_3(N_s)$ that can be added to the series (26) in the form

$$r = r_0 \left(1 - r_1 \frac{\gamma_0}{\sqrt{N_s}} - r_2(N_s) \frac{\gamma_0^2}{N_s} - r_3(N_s) \frac{\gamma_0^3}{N_s^{3/2}} \right), \tag{66}$$

with

$$r_3(N_s) \overset{N_s \gg 1}{\propto} N_s^2 \left[a_3(N_s) - \tilde{a}_3(N_s) \right],$$

where

$$a_3(N_s) \overset{N_s \gg 1}{\propto} -N_s \zeta(3), \quad \tilde{a}_3(N_s) \overset{N_s \gg 1}{\propto} -\frac{C_F}{N_c} N_s \zeta(3). \tag{67}$$

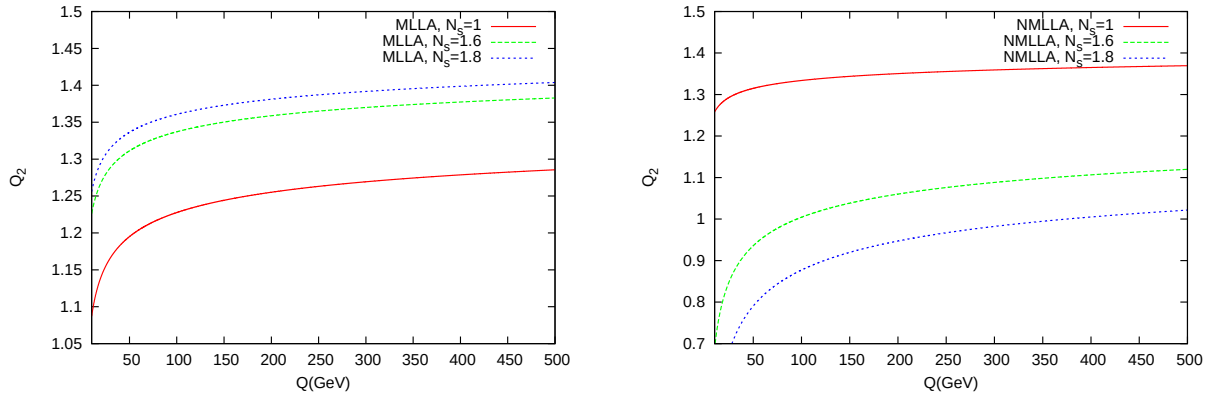

Figure 4: MLLA (41) and NMLLA (63) second multiplicity correlator inside a quark jet as a function of $Q = E\Theta$ in the vacuum ($N_s = 1$) and in the medium ($N_s = 1.6$ and $N_s = 1.8$).

These coefficients follow from (3,4) by further expanding the perturbative series and therefore,

$$-\, r_3(N_s) \overset{N_s \gg 1}{\propto} N_s^3 \left(1 - \frac{C_F}{N_c}\right) \zeta(3) > 0. \tag{68}$$

Thus, replacing $-r_3(N_s) \overset{N_s \gg 1}{\propto} N_s^3$ in (66), the third term changes its sign and therefore, the MLLA trends as $N_s > 1$ can be recovered. However, the whole calculation requires the implementation of the two-loops coupling constant in the solution, and eventually, the inclusion of the time-like sub-leading splitting functions in the evolution equations. Nevertheless, as powers of N_s increase for higher order terms, the perturbative approach fails and the exact numerical solution of the evolution equations becomes necessary.

4 Conclusions

In this paper we have dealt with the medium-modified average multiplicity and the medium-modified second multiplicity correlators in quark and gluon jets. Our calculations are based on the Borghini-Wiedemann model [5], which models parton energy loss in a dense nuclear medium. The average multiplicity is found, after multiple re-scattering of the relativistic hard parton in the medium, to be enhanced by the factor $\sqrt{N_s}$ on the exponential leading contribution. The former leads, in particular, to the medium-modified anomalous dimension γ_{med} ($\gamma \to \gamma_{\text{med}} \approx \sqrt{N_s}\gamma_0$). Corrections to the leading double logarithmic contribution of the average multiplicity arise from both the MLLA and the NMLLA, which better account for the energy balance and for the running of the coupling constant α_s effects as in the vacuum. In particular, the NMLLA average multiplicity distribution is softer at NMLLA than at MLLA (see Fig. 1), such that the available phase space for harder collinear hadronic production becomes restricted. The increase of the average multiplicity at NNLO is driven by the factor $\propto N_s^{3/2}$ (see (23)).

The MLLA scheme provides a more realistic picture of the jet quenching through the study of these observables: such is the case of the medium-modified gluon to quark average multiplicity ratio $r = N_g/N_q$. Indeed, hard corrections are suppressed by the extra factor $1/\sqrt{N_s}$, which leads to restriction on production of hard partons in quark and gluon jets. Therefore, r approaches its asymptotic DLA

limit $r_0 = N_c/C_F = 9/4$ when the coherent radiation of soft gluons is enhanced by the medium. The amplitude of the oscillating series turns out to be wider in the medium than in the vacuum at all energies. Nevertheless, the shapes obtained at MLLA and NMLLA are roughly identical but the series may require the incorporation of higher order corrections. Furthermore, in both approaches, the gluon jets are still more active than the quark jets in producing secondary particles but these characteristics are related to the jet energy dependence of these observables rather than to the sensitivity to the parameter N_s in the nuclear medium.

The second multiplicity correlators in quark and gluon jets in the medium are also computed at MLLA and NMLLA. The multiplicity fluctuations of individual events must be larger for quark jets as compared to gluon jets just like in the vacuum. The MLLA corrections are suppressed by $1/\sqrt{N_s}$, such that A_2 approaches the asymptotic DLA regime as $N_s > 1$, reproducing the expected physics. In addition, the KNO scaling holds at MLLA and NMLLA in heavy-ion collisions, the flattening of the slopes in both the vacuum and the medium is roughly reached for the same virtualities $Q > 100$ GeV of the jet energy. As before, the scaling depends on the energy scale Q rather than on the sensitivity to the nuclear factor N_s. At NMLLA, the behavior as $N_s > 1$ is inverted, but this output can be cured, either by incorporating higher order terms to the series or by exactly solving the evolution equations numerically, but this is out of the scope of this paper.

Finally, our results might lead to more accurate prescriptions for the behavior of these observables in the presence of the nuclear environment if the treatment of parton energy loss is improved in the future. Furthermore, the study of parton energy loss and medium-modified observables would ideally require the re-construction of jets in heavy-ion collisions. Of course, the huge background makes this task highly delicate. Nevertheless, thanks in particular to important theoretical developments on the jet reconstructions algorithms [32] in a high-multiplicity environment, future analysis at the LHC by ALICE [33] and CMS [34] look very promising.

Acknowledgments: I would like to thank B.A. Kniehl for supporting my stay at University of Hamburg, as well as S. Albino, F. Arleo and I. Dremin for enlightening discussions and useful comments on the manuscript.

List of Figures

References

[1] Yu.L. Dokshitzer, V.A. Khoze, A.H. Mueller & S.I. Troyan, Basics of Perturbative QCD, Editions Frontières, Paris (1991).

[2] K. Adcox et al. (PHENIX Collab.), Phys. Rev. Lett. **88** (2002) 022301;
S.S. Adler et al. (PHENIX Collab.), Phys. Rev. Lett. **91** (2003) 072301.

[3] C. Adler et al. (STAR Collab.), Phys. Rev. Lett **89** (2002) 202301.

[4] F. Arleo, hep-ph/08101193;
R. Baier, D. Schiff & B. G. Zakharov, Ann. Rev. Nucl. Part. Sci. **50** (2000) 37;
A. Kovner & U. A. Wiedemann, in Quark Gluon Plasma 3, World Scientific, Singapore, hep-ph/0304151;
M. Gyulassy, I. Vitev, X.-N. Wang & B.-W. Zhang, nucl-th/0302077, ibid.;
A. Majumder, J. Phys. G **34** (2007) S377;
For a more recent review, see also S. Peigné & A.V. Smilga, hep-ph/08105702.

[5] N. Borghini & U.A. Wiedemann, hep-ph/0506218.

[6] N. Armesto, L. Cunqueiro, C. Salgado & W.C. Xiang, JHEP **02** (2008) 048.

[7] S. Sapeta & U.A. Wiedemann, hep-ph/0809.4251.

[8] U.A. Wiedemann, Nucl. Phys. B **588** (2000) 303.

[9] V. N. Gribov & L. N. Lipatov, Yad. Fiz. **15**, 781 (1972) [Sov. J. Nucl. Phys. **15**, (1972) 438]; G. Altarelli & G. Parisi, Nucl. Phys. B **126**, (1977) 298; Yu. L. Dokshitser, Zh. Eksp. Teor. Fiz. **73**, (1977) 1216; [Sov. Phys. JETP **46**, (1977) 641].

[10] A.H. Mueller, Nucl. Phys. B **241** (1984) 141; Erratum ibid., B **241** (1984) 141.

[11] E.D. Malaza & B.R. Webber, Phys. Lett. **B** 149 (1984) 501; E.D. Malaza & B.R. Webber, Nucl. Phys. **B** 267 (1986) 702.

[12] I.M. Dremin & V.A. Nechitailo, Mod. Phys. Lett. A **9** (1994) 1471; JETP Lett. **58** (1993) 945.

[13] I.M. Dremin, C.S. Lam & V.A. Nechitailo, Phys. Rev. D **61** (2000) 074020.

[14] G. Abbiendi et al., [OPAL Collaboration], Phys. Rev. D **69** (2004) 032002.

[15] J. Abdallah et al. [DELPHI Collaboration], Eur. Phys. J. C **44** (2005) 311.

[16] HRS Coll., Phys. Rev. D **34** (1986) 3304; AMY Coll., Phys. Rev. D **42** (1990) 737; DELPHI Coll., Z. Phys. C-Particles and Fields **50** (1991) 185.

[17] I.M. Dremin & J.W. Gary, Phys. Rep. **349** (2001) 301.

[18] D. Acosta et al., Phys. Rev. Lett. **94** (2005) 171802.

[19] A.N. Safonov (for CDF Collaboration), Nucl. Phys. B (Proc. suppl.) **86** (2000) 55.

[20] R. Perez-Ramos, F. Arléo & B. Machet, Phys. Rev. D **78** (2008) 014019; F. Arléo, R. Perez-Ramos & B. Machet, Phys. Rev. Lett. **100** (2008) 052002.

[21] I.M. Dremin, O.S. Shadrin, J. Phys. G **32** (2006) 963.

[22] N. Armesto, C. Pajares & P. Quiroga Arias, hep-ph/0809.4428.

[23] Ya.I. Azimov, Yu.L. Dokshitzer, V.A. Khoze & S.I. Troian, Z. Phys. C **27** (1985) 65; Yu.L. Dokshitzer, V.A. Khoze & S.I. Troian, J. Phys. G **17** (1991) 1585.

[24] R. Perez-Ramos, hep-ph/0811.2418.

[25] V.A. Khoze & W. Ochs, Int. J. Mod. Phys. A **12** (1997) 2949.

[26] S. Sapeta & U.A. Wiedemann, Eur. Phys. J. **C55** (2008) 293.

[27] M. Heinz for the STAR Collaboration, nucl-exp/0809.3769.

[28] Yu.L. Dokshitzer, Phys. Lett. B **305** (1993) 295.

[29] S. Lupia & W. Ochs, Phys. Lett. B **418** (1998) 214.

[30] R. Perez-Ramos, JHEP **06** (2006) 019, and references therein; R. Perez-Ramos, JHEP **09** (2006) 014.

[31] A.M. Polyakov, Sov. Phys. JETP **32** (1971) 296.

[32] M. Cacciari & G.P. Salam, Phys. Lett. B **641** (2006) 57.

[33] ALICE collaboration, B. Alessandro *et al.*, J. Phys. G **32** (2006) 1295.

[34] CMS collaboration, D. d'Enterria (Ed.) *et al.*, J. Phys. G **34** (2007) 2307.